Journal of Nuclear Materials 389 (2009) 332–335

Contents lists available at ScienceDirect

Journal of Nuclear Materials

journal homepage: www.elsevier.com/locate/jnucmat

Anisotropy of disorder accumulation and recovery in 6H–SiC irradiated with Au^{2+} ions at 140 K

W. Jiang *, W.J. Weber

Pacific Northwest National Laboratory, P.O. Box 999, Richland, WA 99352, USA

A B S T R A C T

Single crystal ⟨0001⟩-oriented 6H–SiC was irradiated with Au^{2+} ions to fluences of 0.032, 0.058 and 0.105 ions/nm^2 at 140 K and was subsequently annealed at various temperatures up to 500 K. The relative disorder on both the Si and C sublattices has been determined simultaneously using *in situ* D^+ ion channeling along the ⟨0001⟩ and ⟨2$\bar{2}$01⟩ axes. A higher level of disorder on both the Si and C sublattices is observed along the ⟨2$\bar{2}$01⟩. There is a preferential C disordering and more C interstitials are aligned with ⟨0001⟩. Room-temperature recovery along ⟨2$\bar{2}$01⟩ occurs, which is associated with the ⟨0001⟩-aligned interstitials that annihilate due to close-pair recombination. Disorder recovery between 400 and 500 K is primarily attributed to annihilation of interstitials that are misaligned with ⟨0001⟩ and to epitaxial crystallization. Effects of stacking order in SiC on disorder accumulation are insignificant; however, noticeable differences of low-temperature recovery in Au^{2+}-irradiated 6H–SiC and 4H–SiC are observed.

1. Introduction

Radiation effects in silicon carbide (SiC) have been extensively investigated for over a decade due to its excellent physical and chemical properties that make the material a prominent candidate for a variety of applications. In addition to the fabrication of high-temperature, high-power and high-frequency microelectronic and optoelectronic devices [1], silicon carbide also has been proposed for nuclear applications that include the structural component in fusion reactors [2], cladding material for gas-cooled fission reactors [3] and an inert matrix for the transmutation of plutonium and other transuranics [4]. Previous experimental studies have led to important findings and evidence that significantly improve the knowledge of the physical processes in disorder accumulation, amorphization, microstructural evolution, volume change, defect recovery, and interactions of implanted species in ion-irradiated SiC [5–14]. In a previous report [15], a multiaxial channeling method was used to study the damage states of low-defect concentrations produced by Au^{2+} ion irradiation of 6H–SiC at room temperature. This method allows one to observe displaced atoms from different orientations, which can provide some details about the defect configurations. To minimize the temperature effects on disorder accumulation, irradiation and *in situ* disorder measurements at low temperatures are required. This communication reports on the results for 6H–SiC irradiated at 140 K and isochronally annealed at various temperatures up to 500 K. The results from this study will be discussed and compared to those for 6H–SiC irradiated at room temperature [15], as well as to the data for 4H–SiC irradiated at 165 K [16].

2. Experimental procedure

The 6H–SiC wafer used in this study had a high crystalline quality with the minimum yield (χ_{min}) of ~3%, as determined along the ⟨0001⟩ axis. Three areas on the specimen were irradiated at 140 K with 2 MeV Au^{2+} ions to fluences of 0.032, 0.058 and 0.105 Au^{2+}/nm^2, respectively. A large tilt angle of 60° off the (0001)-surface normal was chosen to produce shallow damage that could be readily measured by *in situ* ion channeling methods. A low ion-beam flux of ~2×10^{11} Au^{2+}/cm^2/s was utilized to minimize the high-dose rate effects on disorder production and to prevent significant beam heating during irradiation. A uniform beam intensity over each of the irradiated areas (3.4×1.9 mm^2) was achieved by using a beam rastering system. Subsequent to irradiation, *in situ* ion channeling analyses were performed using 0.94 MeV D^+ ions along the ⟨0001⟩ and ⟨2$\bar{2}$01⟩ axes that have an included angle of 35.2°. The analyzing beam within the irradiated spot had a typical beam current of ~20 nA and caused negligible damage in the investigated depth region during the channeling measurements. Random-equivalent spectra were obtained at an off-axis orientation (polar angle = 7° relative to ⟨0001⟩ or ⟨2$\bar{2}$01⟩ axis) with rotating flip angles ranging from −3° to +3°. An additional area on the 6H–SiC wafer was fully amorphized to the surface for accurate

* Corresponding author. Tel.: +1 509 371 6491; fax: +1 509 371 6242.
E-mail address: weilin.jiang@pnl.gov (W. Jiang).

0022-3115/$ - see front matter © 2009 Elsevier B.V. All rights reserved.
doi:10.1016/j.jnucmat.2009.02.023

normalization of the random spectra. The charge of the incident beam was integrated by applying a positive voltage of 300 V to the target to suppress the secondary electron emission.

Simultaneous determination of disorder on both the Si and C sublattices in SiC was achieved based on the ⟨0001⟩ and ⟨2$\bar{2}$01⟩ channeling geometries for ^{28}Si(d,d)^{28}Si Rutherford backscattering spectrometry (RBS/C) combined with ^{12}C(d,p)^{13}C nuclear reaction analysis (NRA/C) at a scattering or reaction angle of 150°. The low D^+ ion energy of 0.94 MeV [10,15–17] was selected to improve the depth resolution for profiling narrow disorder distributions in the irradiated specimen. The energy stability of the incident D^+ ions was better than ±3 keV, which is necessary to ensure an accurate analysis of the C sublattice from the (d,p) reaction. *In situ* isochronal annealing was also performed in vacuum at temperatures up to 500 K with an increment of 30–50 K for 20 min each. The same ion-beam methods were employed to analyze the residual disorder in the annealed sample. For samples that were annealed at or below 300 K, the channeling measurements were conducted well below the corresponding annealing temperature; for those annealed above 300 K, measurements were conducted at room temperature (294 K). This procedure is considered to be important to ensure that the disorder recovery processes were quenched during the ion channeling analysis. During both the ion irradiation and channeling measurements, the vacuum in the target chamber was typically in the range of 10^{-6} Pa, and carbon contamination on the sample surface was not observed.

3. Results and discussion

3.1. Disorder accumulation

In situ ⟨0001⟩-aligned spectra for 6H–SiC irradiated at 140 K with 2 MeV Au^{2+} to three ion fluences are shown in Fig. 1. Also included are random and ⟨0001⟩-aligned spectra from an unirradiated area, which, respectively, define the upper and lower levels of the scattering/reaction yields from the amorphous and essentially defect-free SiC. From Fig. 1, the Si damage peaks are readily measurable from the ^{28}Si(d,d)^{28}Si RBS/C. In addition, there are also ^{12}C(d,p)^{13}C NRA/C yields (multiplied by a factor of 4 in Fig. 1) at larger channel numbers, which appear in a background-free region and are completely resolvable from the RBS/C spectra. This condition allows for a simultaneous analysis of disorder on the Si and C sublattices from one measurement. Fig. 2 shows ⟨2$\bar{2}$01⟩-aligned spectra for the same damage states as shown in Fig. 1. Apparently,

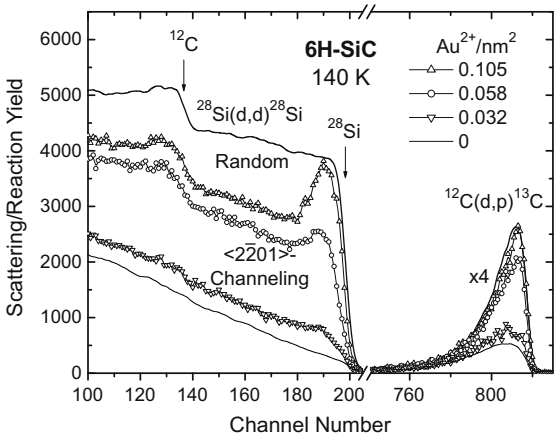

Fig. 2. *In situ* 0.94 MeV D^+ ⟨2$\bar{2}$01⟩-aligned RBS/NRA spectra for (0001)-oriented 6H–SiC irradiated 60° of the surface normal with 2 MeV Au^{2+} ions at 140 K. Also included are random and channeling spectra from an unirradiated area.

the scattering/reaction yields at the damage peak for both sublattices observed along ⟨2$\bar{2}$01⟩ are significantly closer to its random level than those along ⟨0001⟩. This indicates anisotropy of disorder accumulation in 6H–SiC, as will be discussed in detail below. The minimum yield (8%) for the unirradiated 6H–SiC along the ⟨2$\bar{2}$01⟩ is higher than that (3%) along ⟨0001⟩ probably due to pre-existing defects that are aligned with ⟨0001⟩, such as possible micropipes, impurities and point defects.

The relative disorder on the Si and C sublattices has been obtained using a linear dechanneling approximation. This simple method is useful to extract the disorder at the damage peak with comparable precision to an iterative procedure [18–21]. The effects of defect type [22,23], impurities and lattice strain on the dechanneling yields are assumed to be negligible. The accumulated disorder at the damage peak for both the Si and C sublattices, observed along the ⟨0001⟩ and ⟨2$\bar{2}$01⟩ axes is shown in Fig. 3 as a function of dose in units of displacements per atom (dpa). The experimental error shown in the figure has been estimated based on two independent sources [24], i.e., the uncertainty due to the analytical method (5%) and the statistical fluctuation of the data. The dpa values at the damage peak are obtained from the ion fluence multiplied by a factor of 0.6273 obtained based on SRIM simulations [25], where the threshold displacement energies for Si and C sublattices are chosen to be 35 and 20 eV, respectively [26]. In

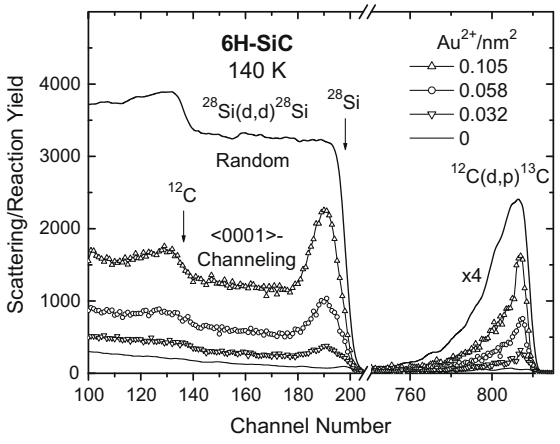

Fig. 1. *In situ* 0.94 MeV D^+ ⟨0001⟩-aligned RBS/NRA spectra for (0001)-oriented 6H–SiC irradiated 60° of the surface normal with 2 MeV Au^{2+} ions at 140 K. Also included are random and channeling spectra from an unirradiated area.

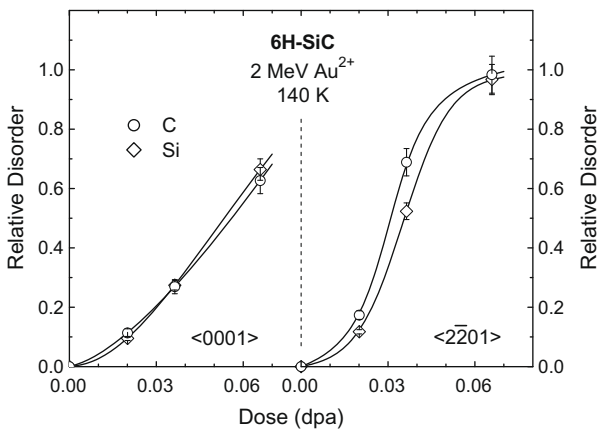

Fig. 3. Relative disorder on the Si and C sublattices, observed along the ⟨0001⟩ and ⟨2$\bar{2}$01⟩ axes, as a function of dose in displacement per atom (dpa) at the damage peak in 6H–SiC irradiated 60° of the surface normal with 2 MeV Au^{2+} ions at 140 K.

general, the accumulated disorder shows a strong orientation dependence. There is a higher level of disorder on both Si and C sublattices along $\langle 2\bar{2}01\rangle$ than $\langle 0001\rangle$ for the same damage states, which suggests that some interstitial defect types in the irradiated SiC are well aligned with the $\langle 0001\rangle$ axis. This behavior is similar to that of 6H–SiC irradiated at room temperature [15] and 4H–SiC irradiated at 165 K [16]. As noted elsewhere [27], the indices for the $\langle 2\bar{2}01\rangle$ axis were incorrectly labeled as $\langle 1\bar{1}02\rangle$ in Ref. [15]. The results in Fig. 3 also indicate a higher level of disorder on the C sublattice than on the Si sublattice along the $\langle 2\bar{2}01\rangle$ axis. The higher C disorder is attributed to a smaller threshold displacement energy on the C sublattice, which is consistent with molecular dynamics (MD) simulations [26] and other experimental measurements [28]. Apparently, more C than Si displacements are aligned with the $\langle 0001\rangle$ axis at 140 K. This behavior is again similar to previous reports on 6H–SiC and 4H–SiC [15,16]. The similarity of disordering behavior may be attributed to the identical local structure of SiC_4 and CSi_4 tetrahedrons in the SiC polytypes.

The excess disorder observed along the $\langle 2\bar{2}01\rangle$ direction relative to that along $\langle 0001\rangle$ is obtained by subtracting the $\langle 0001\rangle$ results from the $\langle 2\bar{2}01\rangle$ results in Fig. 3 at each corresponding dose. This excess disorder is shown in Fig. 4 as a function of dose at the damage peak. The solid lines are the smooth connections of the data points. The relative excess disorder excludes the contribution of three-dimensional interstitial and amorphous clusters that are observable along all axes; thus the results in Fig. 4 are largely representative of the stable interstitial concentrations that are visible along $\langle 2\bar{2}01\rangle$, but not along $\langle 0001\rangle$. These defects may be in the form of single interstitials, the split interstitial (dumbbell) defects as predicted by *ab initio* results [29]], and/or other types of defects that were aligned with the $\langle 0001\rangle$ axis. The results in Fig. 4 indicate that the concentration of the excess C interstitials (~0.42) along $\langle 2\bar{2}01\rangle$ is higher than that of the excess Si interstitials (~0.27) at 0.04 dpa. After the concentrations are maximized or saturated, they are expected to decrease with the increasing dose and vanish at the critical dose for amorphization (0.12 dpa at 150 K [30]).

3.2. Disorder recovery

The general behavior of disorder recovery in Au^{2+} irradiated 6H–SiC observed along the $\langle 0001\rangle$ axis has been reported [10]. Since there are considerable shielding effects of the $\langle 0001\rangle$ atomic rows on some types of irradiation-induced defects, as discussed above, studies of defect recovery along other axes might lead to important insights, as indicated in an early study of 6H–SiC [15], where only one annealing temperature (570 K) was used.

The isochronal annealing data at various temperatures for 20 min each are shown in Figs. 5 and 6, representing the results observed along the $\langle 0001\rangle$ and $\langle 2\bar{2}01\rangle$ axes, respectively. In general, the recovery of disorder is both sublattice and orientation dependent. At the lowest ion fluence (0.032 Au^{2+}/nm^2), there is only a modest recovery of disorder on the Si sublattice observed along $\langle 0001\rangle$ at 190 K and along $\langle 2\bar{2}01\rangle$ at 300 K. Slightly more recovery on the C sublattice occurs along both the $\langle 0001\rangle$ and $\langle 2\bar{2}01\rangle$ axes at 190 and 300 K, respectively. Thermal annealing at higher temperatures up to 500 K does not lead to a significant recovery. The damage states in the as-irradiated specimen at the lowest dose are expected to contain isolated point defects and possibly a few defect clusters. The defect recovery at the low temperatures is primarily associated with close-pair recombination, as suggested by recent kinetic lattice Monte Carlo simulations of damage annealing in 3C–SiC [31]. The probability for combination of uncorrelated interstitials and vacancies, which happens at higher temperatures, is small due to the low concentration of point defects.

From Fig. 6, a recovery stage for both the Si and C sublattices at 0.058 Au^{2+}/nm^2 is observed along $\langle 2\bar{2}01\rangle$ between 190 and 300 K. This disorder recovery is again attributed to close-pair recombination [31]. The absence of this recovery for the same damage states when observed along the $\langle 0001\rangle$ direction in Fig. 5 indicates that the annihilated Si and C interstitials were well aligned with the $\langle 0001\rangle$ axis. This behavior of the defect recovery was not observed along the $\langle \bar{4}40\bar{3}\rangle$ axis in 4H–SiC irradiated to 0.053 Au^{2+}/nm^2 at 165 K [16]. Since the $\langle 2\bar{2}01\rangle$ direction in 6H–SiC is equivalent to $\langle \bar{4}40\bar{3}\rangle$ in 4H–SiC (both of which have the same angle of ~35.2° relative to $\langle 0001\rangle$), the results in Figs. 5 and 6 indicate that the stacking order of the Si/C double layers in the SiC crystal structures has observable effects on the disorder recovery processes near room temperature. It still remains to be investigated how the atomic arrangements beyond the first nearest neighbors of the point defects affect the configuration and stability of the close-pairs in SiC. The defect recovery above 350 K is due to interstitial migration and epitaxial recrystallization (see below). At this stage, there is a similar recovery rate on the Si sublattice observed along the $\langle 0001\rangle$ and $\langle 2\bar{2}01\rangle$, indicating that a majority of the defect recovery is associated with the annihilation of interstitials that are misaligned with the $\langle 0001\rangle$ axis. It is also interesting to point out that in contrast to a slight reduction in the level of C disorder observed along $\langle 0001\rangle$ from 140 to 190 K, there is a flat level of the C disorder along $\langle 2\bar{2}01\rangle$ within the experimental error. The results may indicate that some of the C interstitials that were

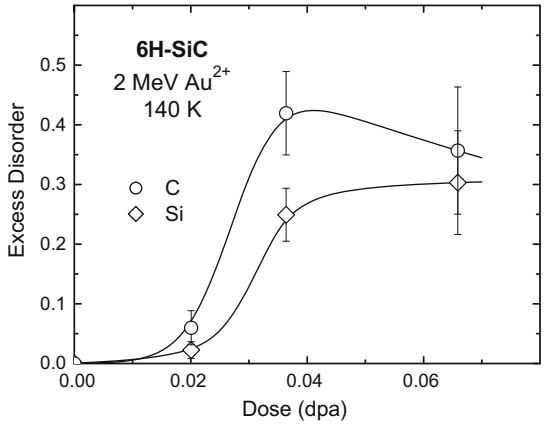

Fig. 4. Relative disorder along $\langle 2\bar{2}01\rangle$ subtracted from the disorder along $\langle 0001\rangle$ as a function of dose (dpa) at the damage peak in 6H–SiC irradiated 60° of the surface normal with 2 MeV Au^{2+} ions at 140 K.

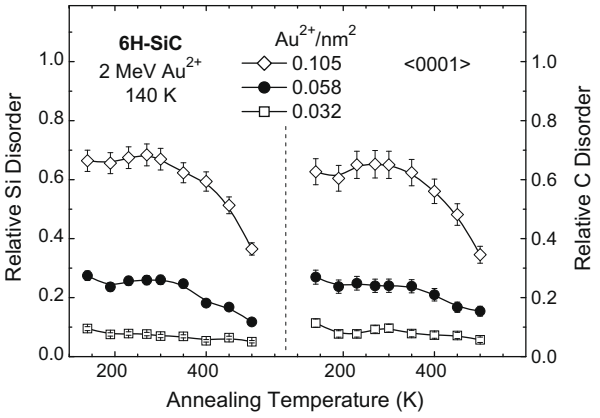

Fig. 5. *In situ* isochronal recovery (20 min) of relative disorder on the Si and C sublattices at the damage peak, observed along the $\langle 2\bar{2}01\rangle$ axis in 6H–SiC irradiated 60° of the surface normal with 2 MeV Au^{2+} ions at 140 K.

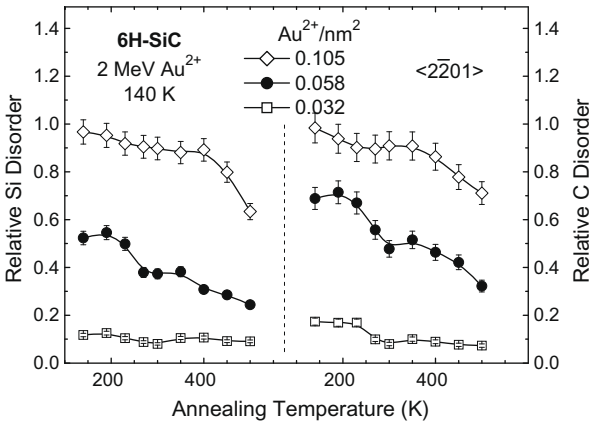

Fig. 6. *In situ* isochronal recovery (20 min) of relative disorder on the Si and C sublattices at the damage peak, observed along the ⟨2$\bar{2}$01⟩ axis in 6H–SiC irradiated 60° of the surface normal with 2 MeV Au^{2+} ions at 140 K.

misaligned at 140 K tend to align with the ⟨0001⟩ axis during lattice relaxation at 190 K.

At the highest fluence (0.105 Au^{2+}/nm^2), point defects are abundant in the irradiated 6H–SiC; in addition, defect complexes are formed in the damage-overlapping processes. These damage states determine the recovery behavior. From Figs. 5 and 6, defect recovery on both Si and C sublattices is minimal below 350 K. However, significant recovery between 400 and 500 K occurs along both ⟨0001⟩ and ⟨2$\bar{2}$01⟩, which is consistent with the previous recovery stage observed for Au^{2+}-irradiated 6H–SiC [10] and with the results for 4H–SiC [16]. The data in Figs. 5 and 6 suggest that the recovery stage is largely associated with the annihilation of interstitials that are misaligned with ⟨0001⟩. This recovery stage could be associated with the uncorrelated annihilation of mobile interstitials that are combined with vacancies, as reported by a recent study [31]. It may be also possible that the epitaxial recrystallization of defect clusters or amorphized zones contributes to the disorder recovery, as has been observed in an earlier study [24]. Further analysis of the data for the fluences of 1.05 and 0.058 Au^{2+}/nm^2 in Figs. 5 and 6 reveals that at temperatures between 270 and 500 K, there is a significantly higher level of ⟨0001⟩-aligned Si displacements than C (0.25 vs. 0.12) for the higher fluence; however, the aligned C displacements for the two fluences have a comparable level (0.26) between 300 and 500 K.

4. Summary

Damage accumulation and recovery in 6H–SiC irradiated with Au^{2+} ions at 140 K have been studied *in situ* using D^+ channeling along the ⟨0001⟩ and ⟨2$\bar{2}$01⟩ axes. There is a strong orientation dependence of disorder accumulation and recovery. A higher level of disorder on both the Si and C sublattices is observed along the ⟨2$\bar{2}$01⟩ axis. More C displacements are aligned with the ⟨0001⟩ axis. The aligned displacements may include single interstitials and split interstitial defects. In addition, there is a preferential disordering rate on the C sublattice, which is attributed to a smaller threshold displacement energy on the C sublattice. The disordering behavior of 6H–SiC is similar to that of 4H–SiC under similar irradiation conditions, probably due to the identical local atomic arrangements (SiC_4 and CSi_4 tetrahedrons) in the SiC polytypes. Lattice relaxation at 190 K is observed in 6H–SiC irradiated to 0.058 Au^{2+}/nm^2 at 140 K, leading to alignment of displaced C atoms with the ⟨0001⟩ axis. The recovery at room temperature is largely associated with the annihilation of the ⟨0001⟩-aligned interstitials in close-pair recombination. This behavior was not observed in 4H–SiC irradiated and annealed under similar conditions. The difference could originate from the effects of stacking order in SiC on the configuration and stability of close Frenkel pairs. During thermal annealing at temperatures between 400 and 500 K, significant recovery of disorder on both the Si and C sublattices is observed in 6H–SiC irradiated to 0.058 and 1.05 Au^{2+}/nm^2, which is mostly attributed to the annihilation of interstitials that are misaligned with ⟨0001⟩ and to the epitaxial recrystallization of defect clusters and amorphized zones.

Acknowledgements

This research was supported by the Division of Materials Sciences and Engineering, Office of Basic Energy Sciences, U.S. Department of Energy under Contract DE-AC05-76RL01830. Support for the accelerator facilities within the Environmental Molecular Sciences Laboratory (EMSL) at the Pacific Northwest National Laboratory (PNNL) was provided by the Office of Biological and Environmental Research, U.S. Department of Energy.

References

[1] C. Raynaud, J. Non-Cryst. Solid 280 (2001) 1.
[2] P. Fenici, A.J. Frias Rebelo, R.H. Jones, A. Kohyama, L.L. Snead, J. Nucl. Mater. 258–263 (1998) 215.
[3] B.G. Kim, Y. Choi, J.W. Lee, Y.W. Lee, D.S. Sohn, G.M. Kim, J. Nucl. Mater. 281 (2000) 163.
[4] R.A. Verrall, M.D. Vlajic, V.D. Krstic, J. Nucl. Mater. 274 (1999) 54.
[5] S.J. Zinkle, L.L. Snead, Nucl. Instrum. and Meth. B 116 (1996) 92.
[6] W.J. Weber, L.M. Wang, N. Yu, N.J. Hess, Mater. Sci. Eng. A 253 (1998) 62.
[7] E. Wendler, A. Heft, W. Wesch, Nucl. Instrum. and Meth. B 141 (1998) 105.
[8] W. Jiang, W.J. Weber, S. Thevuthasan, R. Grötzschel, Nucl. Instrum. and Meth. B 166&167 (2000) 374.
[9] W.J. Weber, W. Jiang, S. Thevuthasan, Nucl. Instrum. and Meth. B 166&167 (2000) 410.
[10] W. Jiang, W.J. Weber, S. Thevuthasan, V. Shutthanandan, J. Nucl. Mater. 289 (2001) 96.
[11] Y. Zhang, W.J. Weber, W. Jiang, C.M. Wang, V. Shutthanandan, A. Hallén, J. Appl. Phys. 95 (2004) 4012.
[12] W. Jiang, Y. Zhang, V. Shutthanandan, S. Thevuthasan, W.J. Weber, Appl. Phys. Lett. 89 (2006) 261902.
[13] W. Jiang, Y. Zhang, M.H. Engelhard, W.J. Weber, G.J. Exarhos, J. Lian, R.C. Ewing, J. Appl. Phys. 101 (2007) 023524.
[14] W. Jiang, P. Nachimuthu, W.J. Weber, L. Ginzbursky, Appl. Phys. Lett. 91 (2007) 091918.
[15] W. Jiang, W.J. Weber, Phys. Rev. B 64 (2001) 125206.
[16] Y. Zhang, F. Gao, W. Jiang, D.E. McCready, W.J. Weber, Phys. Rev. B 70 (2004) 125203.
[17] W. Jiang, W.J. Weber, S. Thevuthasan, R. Grötzschel, Nucl. Instrum. and Meth. B 161–163 (2000) 501.
[18] J.S. Williams, R.G. Elliman, Channeling, in: J.R. Bird, J.S. Williams (Eds.), Ion Beams for Materials Analysis, Academic, San Diego, 1989, p. 286.
[19] M.L. Swanson, Channeling, in: J.R. Tesmer, M. Nastasi (Eds.), Handbook of Modern Ion Beam Materials Analysis, Materials Research Society, Pittsburgh, 1995, p. 267.
[20] W. Jiang, W.J. Weber, C.M. Wang, L.M. Wang, K. Sun, Defect Diffus. Forum 226–228 (2004) 91.
[21] Y. Zhang, W.J. Weber, V. Shutthanandan, S. Thevuthasan, Nucl. Instrum. and Meth. B 251 (2006) 127.
[22] W.K. Chu, J.W. Mayer, M.A. Nicolet, Backscattering Spectrometry, Academic, New York, 1978.
[23] L.C. Feldman, J.W. Mayer, S.T. Picraux, Materials Analysis by Ion Channeling, Academic Press, New York, 1982.
[24] W. Jiang, W.J. Weber, S. Thevuthasan, D.E. McCready, Surf. Interface Anal. 27 (1999) 179.
[25] J.F. Ziegler, J.P. Biersack, U. Littmark, The Stopping and Range of Ions in Solids, Pergamon, New York, 1985.
[26] R. Devanathan, W.J. Weber, F. Gao, J. Appl. Phys. 90 (2001) 3203.
[27] W. Jiang, W.J. Weber, Experimental studies of defects, implants, and their processes in ion-irradiated silicon carbide single crystals, in: S.G. Pandalai (Ed.), Recent Research Development in Applied Physics, vol. 6, Part II, Transworld Research Network, Kerala, 2003 (Chapter 19).
[28] S.J. Zinkle, C. Kinoshita, J. Nucl. Mater. 251 (1997) 200.
[29] F. Gao, E.J. Bylaska, W.J. Weber, L.R. Corrales, Phys. Rev. B 64 (2001) 245208.
[30] W. Jiang, Y. Zhang, W.J. Weber, Phys. Rev. B 70 (2004) 165208.
[31] Z. Rong, F. Gao, W.J. Weber, G. Hobler, J. Appl. Phys. 102 (2007) 103508.